



**Department of Electrical and Computer Engineering
National University of Singapore**

**EE5441 Introduction to Nanoelectronics and Emerging Devices
(Semester II, AY2023/2024)**

Topic - Metallic Quantum well

Purva D. Sute - A0260105X

1. Abstract

This paper explores the significant advancements in nonlinear optics enabled by metallic quantum wells (MQWs). It begins by examining the breakthrough in achieving large second-order optical nonlinearities at visible/near-infrared (NIR) frequencies by introducing a metal/dielectric heterostructured platform.

Subsequently, the study delves into the enhanced second-order nonlinear effect in asymmetric metallic quantum wells, highlighting the role of intersub-band transitions in achieving large optical nonlinearities. This advancement opens avenues for the development of plasmonic material platforms with superior optical nonlinearities.

The transformative potential of metallic quantum wells in nonlinear optics offer insights into their applications and future directions in the field.

2. Introduction

2.1 What is Metallic Quantum well?

A metallic quantum well is a nanostructure where thin layers of metal are sandwiched between layers of insulating materials. These insulating layers act as potential barriers, confining the motion of electrons within the metallic layers. This confinement has a significant impact on the electronic and optical properties of the metal, leading to unique behaviors compared to bulk metals.

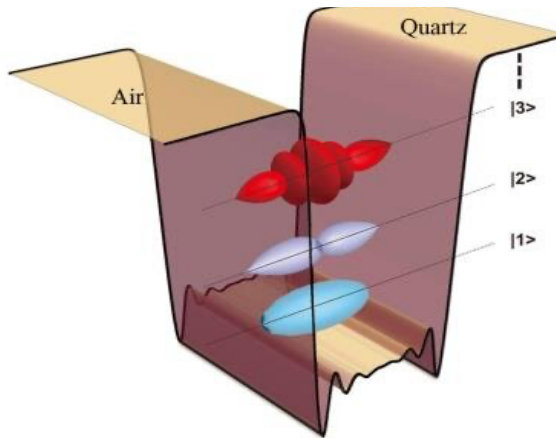


Figure 1: A metal quantum well features an ultrathin gold film between quartz and air

2.2 Importance of metallic quantum wells in nonlinear optics:

The field of nonlinear optics explores how light interacts with materials in a non-linear way, meaning the intensity of the light affects the material's response.

Key Advantages of MQWs in Nonlinear Optics:

- Compared to bulk metals, MQWs exhibit significantly stronger interactions with light. This is a consequence of quantum confinement, which modifies the electronic structure and creates conditions for more efficient light-matter interaction.
- By adjusting the thickness and materials used in the MQW, we can tailor the energy gap between electron energy levels. This allows for designing MQWs that resonate efficiently with specific wavelengths of light, enhancing the nonlinear effects.
- MQWs can support localized surface plasmon resonances, where collective electron oscillations occur at the interface between the metal and insulator layers. These resonances can further amplify light-matter interaction and enable stronger nonlinear effects.

2.3 Overview of the experimental focus

Achieving large second-order optical nonlinearity in the infrared frequency range by utilizing electronic intersubband transitions in semiconductor quantum well heterostructures and exploring transition metal nitrides, particularly titanium nitride to create epitaxial heterostructures with ultra-large second-order susceptibility $\chi^{(2)}$ in the visible to NIR spectra.

Subsequently, achieving a large second-order nonlinear effect in metallic quantum wells, particularly in Au-based asymmetric metallic QWs by Enhancing the intrinsic nonlinear susceptibilities of plasmonic materials by developing quantum-sized metal films on dielectric substrates and Fabricating ultrathin Au metallic QWs with varying asymmetry between insulator pairs to demonstrate a record high second-order susceptibility in the visible to NIR spectral range.

3. Experiment Method

3.1 The research explores a new material platform, metallic coupled quantum wells (cMQWs), for achieving giant second-order optical nonlinearity $\chi^{(2)}$ of 1500 pm/V in the visible/NIR range.

Materials used are -

- Metallic Quantum Wells (cMQWs): They consist of alternating layers of TiN and Al₂O₃ fabricated epitaxially (layer-by-layer growth) using reactive magnetron sputtering. These materials were chosen due to their suitability for epitaxial growth and their desired optical and structural properties. TiN is selected for its plasmonic characteristics, while Al₂O₃ serves as a dielectric barrier between the metallic layers. The specific thicknesses of TiN and Al₂O₃ layers were chosen to achieve a desired double transition frequency for efficient light interaction.
- Substrate: Sapphire was used as the substrate for the cMQW growth.

Fabrication Methods:

- Design: Design the quantum well heterostructure consisting of TiN/Al₂O₃ epitaxial multilayers to create coupled metallic quantum wells.

The cMQWs were carefully designed to support three electronic sub-bands with equal energy spacing (i.e., $E_i - E_{i-1} = E_{i+1} - E_i = \hbar\Omega$, where Ω is the double transition frequency), such that $\chi^{(2)}$ near the Ω is

$$X^2(\omega) = \frac{n(i-1) - ni * e^3 z i - 1, i z i, i + 1 z i + 1, i + 1}{\hbar^2 \epsilon_0 * (\omega - \Omega - i\tau i, i - 1)(2\omega - 2\Omega - i\tau i + 1, i - 1)} \quad \dots \quad (1)$$

- Epitaxial Growth of cMQWs: Reactive magnetron sputtering was used to deposit alternating layers of TiN and Al₂O₃ with precise control over thickness.

Characterization Technique:

- Transmission Electron Microscopy (TEM): As shown in figure 2b, it is used to image the cross-section of the cMQWs and verify the uniformity and thickness of the metallic and dielectric layers.
- SHG Measurement: A pulsed laser beam (fundamental frequency) was used to excite the cMQW. The emitted light was analyzed to detect the presence and intensity of the SHG. The dependence of SHG intensity on incident power was measured.

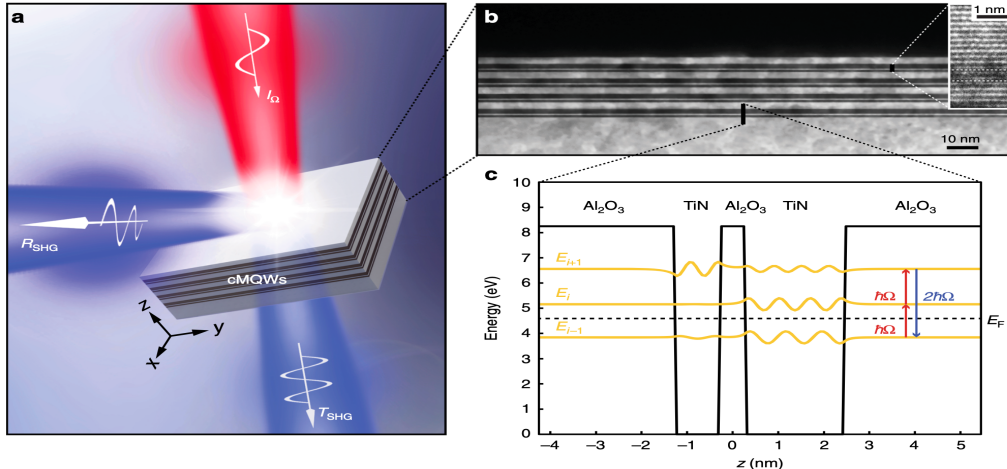


Figure 2 : cMQWs for extreme optical nonlinearities and highly efficient visible-frequency SHG

Experimental Analysis:

- SHG measurements are performed using 100-fs pulse width, 80 MHz repetition rate laser pulses for SHG excitation to characterize the nonlinear optical properties of the fabricated cMQWs. A 50 \times objective lens (NA = 0.8, Olympus IX81) is employed to focus the incident pulse and collect the emitted SHG signals, enabling the determination of the second-order nonlinear susceptibility $\chi^{(2)}$.

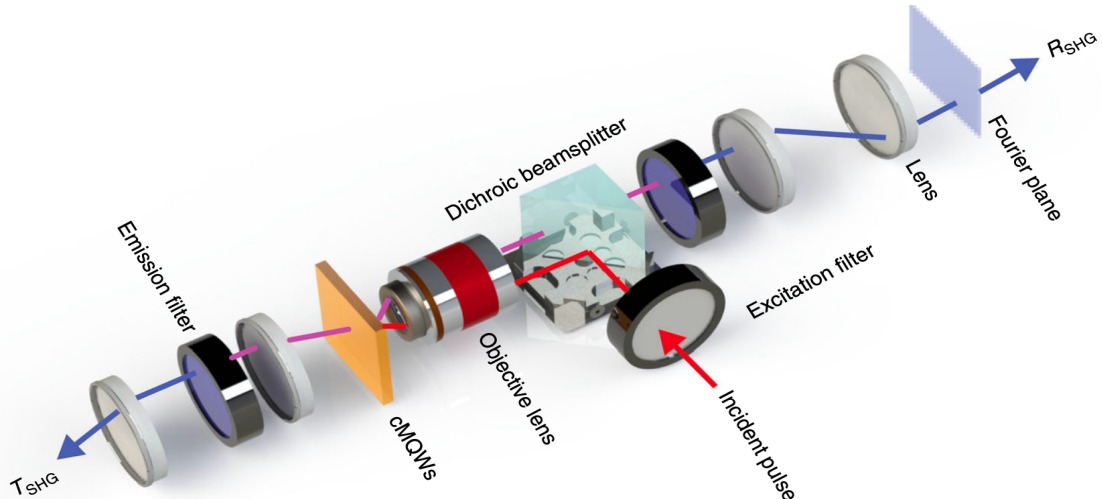


Figure 3 : Schematic diagram of the SHG measurement

- Incident power of the pulsed laser was measured using a power meter to ensure consistent and controlled experimental conditions.
- Excited SHG emission power was collected on both transmission and reflection sides by a photon counting detector.
- Angular SHG emission distribution was acquired at the Fourier plane with a charge-coupled device (CCD; Andor iXon EMCCD).
- Due to the polarization selection rule of intersubband transitions in a planar QW structure, only the electric field component E_z of the pump light contributes to the optical responses of the QW, including the SHG.

Keeping fixed incident angle of $\theta = 30^\circ$ and in-plane polarized pump light with a polarization angle $\varphi = 90^\circ$, samples with a single cMQW unit were investigated to verify the origin of SHG. The sample was excited by a 920-nm (Ω) light pulse with an average power of 3 mW. The measured emission spectrum reflected from the sample exhibits a sharp peak centered at the SHG wavelength of 460 nm (2Ω). This observation confirms

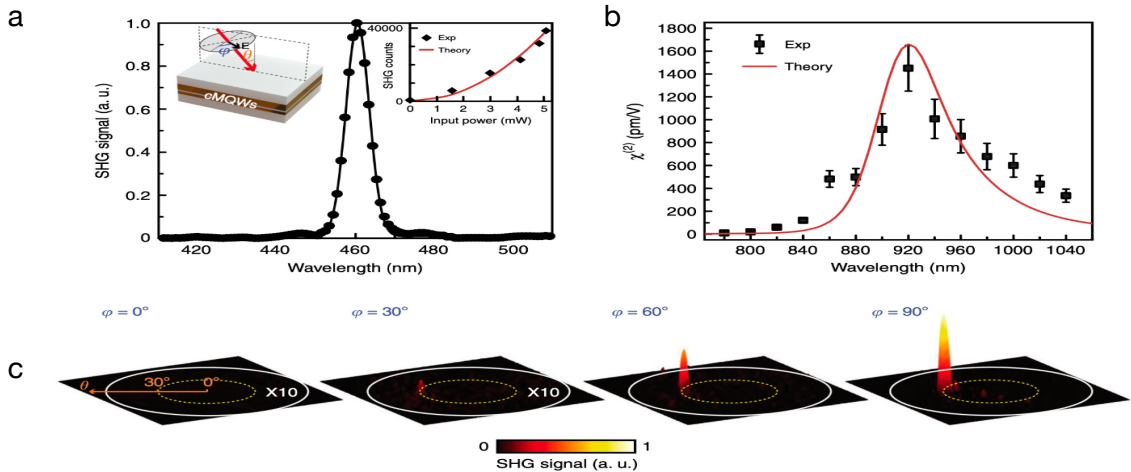


Figure 4 **a.** SHG emission spectrum. **b.** Wavelength dependence of $\chi^{(2)}$ for a single unit of the cMQWs. **c.** CCD images at the back-aperture plane of the objective

the generation of SHG at the expected wavelength. The SHG signals from the substrate and the thick TiN film (30 nm) are below the noise floor under the same experimental conditions. This suggests that the observed SHG signal predominantly originates from the cMQW structure.

Figure 4c shows back-aperture images captured at four different incident polarization states, ranging from out-of-plane ($\varphi = 0^\circ$) to in-plane ($\varphi = 90^\circ$). These images provide insight into the polarization-dependent characteristics of the SHG signals emitted from the sample. In the back-aperture plane, the SHG signals show a prominent peak located at the collection angle of $\theta = 30^\circ$. This localization indicates the directionality of the SHG emission, which aligns with the reflection of the incident light. Under pulse excitation with a peak intensity of 0.48 GW/cm^2 , the SHG emission demonstrates a $\sin^4(\varphi)$ dependence on the incident polarization angle φ . This dependence arises from the intersubband transition polarization selection in quantum well structures. The $\sin^4(\varphi)$ dependence arises because SHG from an intersubband transition is proportional to the square of the out-of-plane polarization intensity I_z , which scales as $E^2 \sin^2(\varphi)$. This indicates how the polarization state of the incident light influences the intensity of the SHG signal.

Experimental and Theoretical Comparison: Fig. 4b presents an experimental comparison between the experimentally obtained $\chi^{(2)}$ spectrum and the theoretical prediction from Equation (1). The $\chi^{(2)}$ spectrum exhibits a resonant peak centered at the double transition frequency Ω (920 nm). This resonance indicates the enhancement of intersubband resonant transitions by the cMQWs. At the near-infrared frequency, the $\chi^{(2)}$ value is exceptionally high, reaching 1500 pm/V. This value is significantly higher than that of traditional nonlinear crystals (such as LiNbO_3) and typical metal structures, making cMQWs promising for ultracompact nonlinear components.

The subsequent study builds upon the investigations detailed earlier, delving into the implications of structural asymmetry on the nonlinear optical properties observed in metallic quantum wells. It extends the research conducted in the previous work by exploring how varying structural configurations affect second-order nonlinear optical behavior. Both inquiries share common methodologies and theoretical frameworks, collectively contributing to a more comprehensive understanding of the nonlinear optical potential of metallic quantum wells.

3.2 This research explores a novel design for achieving a large second-order nonlinearity in commonly used plasmonic metals like Au.

Materials used are -

- Gold (Au) to create metallic quantum wells for nonlinear optical applications.
- Silicon Dioxide (SiO_2) as barrier layers between Au layers in the MQWs.
- Aluminum Oxide (Al_2O_3) used as a barrier layer.
- Hafnium Oxide (HfO_2) employed as a capping layer in the MQW structure.

Substrate

- Sapphire: Provides a stable base for the fabrication of MQWs.
- Silicon (Si): Likely used as a substrate for some fabrication processes.

Fabrication Process:

1. Simulation: A quantum electrostatic model is used to simulate the eigenstates and wavefunctions of electrons in three different Au QW designs with varying structural and chemical asymmetry [Figs. 5(a)–5(c)].

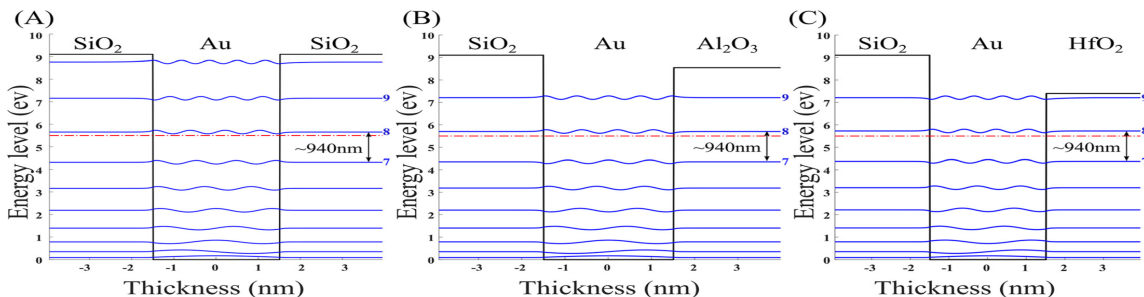


Figure 5 : Conduction band diagrams

2. Device Fabrication (Single QW Unit):

The $\chi^{(2)}$ of these asymmetric metallic QWs was calculated with perturbation theory along the growth direction (z-axis)

$$X_{zzz} \chi^{(2)}(2\omega, \omega, \omega) = \frac{N}{\hbar^2 \epsilon_0} P_f \sum m n \frac{\mu g n * \mu n m * \mu m g}{(\omega n g - 2\omega)(\omega m g - \omega)}$$

$\chi^{(2)}$ becomes nonzero when the QW barrier potential is asymmetric because the dipole transition moment is an integral of an odd function. The barrier asymmetries then induce an asymmetric wavefunction making second- order effects possible in the wells. The wavefunction asymmetry in these wells can be described with a figure of merit because it is hard to discern visually. The FoM shows a clear decrease for increasing asymmetry of the structures over all energy levels and a marked decrease in the maximally asymmetric well structure as compared with the symmetric and medium asymmetry structures. Three single QW unit devices were constructed following simulation in order to achieve these structure. A resonance at the wavelength of 940 nm was targeted with three geometries of increasing chemical and structural asymmetry:

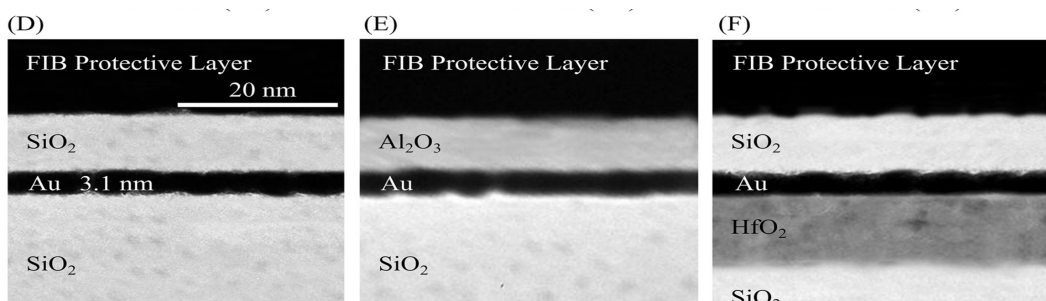


Figure 6. TEM images of QW devices (d) without, (e) with intermediate, and (f) with maximal structural and chemical asymmetry between barrier layers.

Symmetric: Au layer sandwiched between two SiO₂ layers, Intermediate Asymmetry: Au layer between Al₂O₃ capping layer and SiO₂ substrate, Maximal Asymmetry: Au layer between SiO₂ capping layer and HfO₂ substrate

- All oxide barrier layers are around 10 nm thick.
- Au films are around 3.1 nm thick and deposited using a DC sputter system.
- Oxide layers are deposited using either RF sputter system (SiO₂, Al₂O₃) or Atomic Layer Deposition (HfO₂).
- Transmission electron microscopy is used to image the nanofilms after preparation via focused ion beam (FIB) lift-out method.

$\chi^{(2)}$ in a real material may be determined by measurement of a second-order nonlinear process, such as SHG

Characterization Method:

- Second Harmonic Generation (SHG):

SHG measurements are performed to quantify the second-order nonlinear susceptibility of the fabricated MQW samples. A MaiTai pulsed laser system is used to provide illumination at a fixed wavelength, and SHG emission is collected using a photon detector. The SHG signal is calibrated using a known nonlinear material (β -BaB₂O₄ crystal) to determine the $\chi^{(2)}$ values of the MQW samples.

- Power Dependence Measurement:

The power dependence of the SHG signal intensity is measured to assess the contributions of second and third order nonlinear effects. Incident laser power is varied, and the corresponding SHG intensity is recorded using a photon counting detector.

- Transmission Electron Microscopy (TEM):

TEM imaging is performed to visualize the fabricated MQW structures with nanometer resolution. The quality of the MQW layers and interfaces is assessed through TEM images.

Experimental Procedure:

1. SHG Measurement Setup:

- A MaiTai pulsed laser system with 100 fs pulse duration, 80 MHz repetition rate, and 10 mW average power is used for illumination.
- The laser light is focused onto the sample with a spot size of 2 μ m.
- Reflected light is collected using an objective lens and filtered to isolate the SHG signal
- A photon counting detector measures the SHG emission intensity.

2. SHG Spectra Collection:

- The emission wavelength of the sample is scanned from 490 to 510 nm while illuminated with a fixed incident wavelength centered at 1000 nm.
- The SHG spectrum is recorded, showing a peak at the doubled frequency.
- The β -BaB₂O₄ (BBO) crystal with a known $\chi^{(2)}$ is used to calibrate the system for accurate $\chi^{(2)}$ measurement in the Au QW samples.

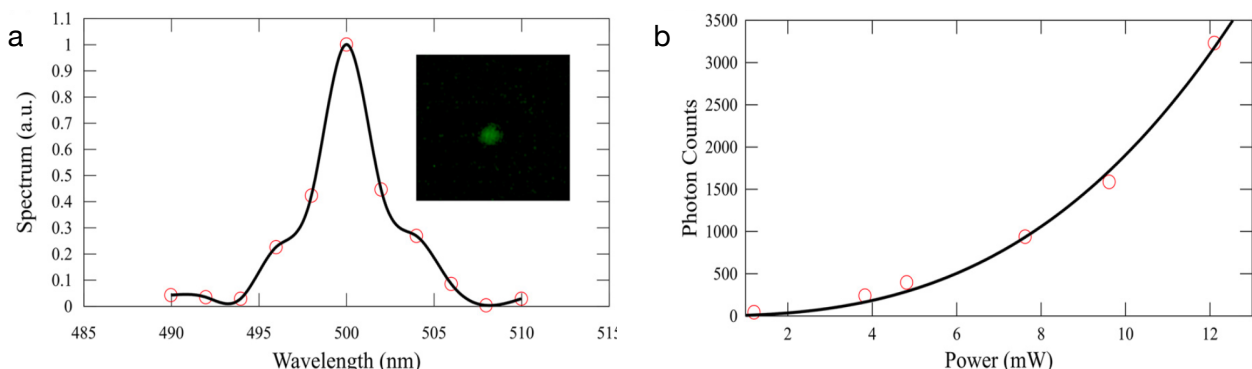


Figure 7 : a. Spectrum as a function of wavelength. b. Power-dependent SHG signal from the maximally asymmetric QW.

3. Power Dependence Measurement:

- The incident light power is varied, and the corresponding SHG signal intensity is measured. This helps differentiate between the contributions of second-order and third-order nonlinearities to the overall signal.

Fig 7b shows the power dependence of signal fitted to a sum of power functions of the form $ax^2 + bx^3$ with factors $a=6:458$, and $b=1:26$ indicating that 83.67% of the total signal intensity resulted from SHG

4. Data Analysis:

- The peak SHG intensity is compared across the different QW designs.
- Equation (2) is used to calculate the effective wavelength-dependent $\chi^{(2)}$ based on the measured SHG intensity, peak excitation pulse intensity, refractive indices at the fundamental and doubled frequencies, speed of light, vacuum permittivity, and interaction length within the QW.

$$X^2 = \sqrt{\frac{2 * I_2\omega * n_2\omega * n_w^2 * c^3 * \epsilon_0}{I^2\omega * \omega^2 * l^2}} \quad \text{--- (2)}$$

Calculated $\chi^{(2)}$ spectra are compared with simulation results are they are relatively similar.

Large second-order optical nonlinearity $\chi^{(2)}$ has been achieved in Au-based quantum wells through electronic intersubband transitions. The asymmetry of metallic QWs is found to correlate with an increase in $\chi^{(2)}$. A significant $\chi^{(2)}$ value of approximately 229.6 pm/V is demonstrated in the near-infrared region around 940 nm wavelength for highly asymmetric QWs.

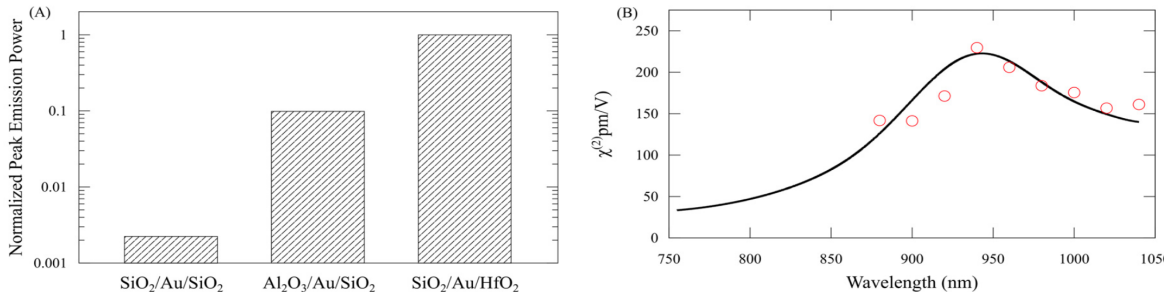


Figure 8 : a. Normalized peak emission power. b. Magnitude of $\chi^{(2)}$ as a function of wavelength.

4. Key Findings

(TiN/Al₂O₃ cMQWs):

- Achieved exceptionally high second-order optical nonlinearity $\chi^{(2)}$ in the near-infrared range through the use of asymmetric coupled metallic quantum wells (cMQWs).
- The precise design of the cMQWs supports resonant enhancement of $\chi^{(2)}$ near the double transition frequency, leading to efficient SHG at visible frequencies from NIR excitation. This demonstrates directionality and auto-phase matching capabilities.

(Asymmetric Au QWs):

- Set a record for high second-order nonlinear susceptibility $\chi^{(2)}$ in asymmetric gold metallic quantum wells, with significant enhancement observed at a 940 nm wavelength.
- This enhancement was achieved by varying the degrees of asymmetry in the quantum well barrier layers, with theoretical models and simulations used to predict and optimize the $\chi^{(2)}$ values.
- Fabrication and characterization of MQW samples with increasing asymmetry were conducted, utilizing TEM imaging and SHG measurements to validate the experimental

results. These showed clear SHG peaks, confirming the high potential of these materials for applications in on-chip nonlinear optical devices.

5. Interpretation of the results

Researchers have significantly advanced the field of nonlinear optics by designing coupled metallic quantum wells achieving exceptionally high second-order optical nonlinearity $\chi^{(2)}$ that surpasses that of traditional materials. In TiN/Al₂O₃ MQWs, the engineering of three subbands with equal energy spacing amplified the nonlinear response due to a strong resonance effect.

Separately, asymmetric Au metallic quantum well structures achieved a record-high $\chi^{(2)}$ of approximately 229.6 pm/V at a 940 nm wavelength, as measured via SHG. This high nonlinearity results from the synergy between electronic intersubband transitions and the asymmetry in the quantum well design, with an increase in QW asymmetry leading to a stronger SHG signal.

6. Limitations of the experimental method

- Additional characterization techniques beyond SHG measurement may be necessary to fully comprehend the underlying physics of nonlinear optical processes in cMQWs.
- Integrating cMQWs into metasurfaces poses challenges regarding precise alignment and optimization of the metasurface structure, requiring further experimental efforts to maximize SHG efficiency.
- The power dependence of the measured signal suggests a combination of second-order and third-order nonlinearities. The effective $\chi^{(2)}$ value might be slightly overestimated due to the unaccounted third-order contribution to the SHG peak.
- The measured SHG signal likely contains contributions from third-order effects as well. The power dependence of the signal deviates from the expected value for pure SHG. The authors separate the contributions by fitting the data to a combined power function considering both second and third-order terms. However, this estimation might not be perfect.

7. Future prospects of related research

- Tailoring quantum states of CMQWs enables high $\chi^{(2)}$ at various wavelengths, facilitating broadband efficient SHG by stacking multiple CMQW layers.
- Combining materials with high $\chi^{(2)}$ and $\chi^{(3)}$ in a single platform offers versatility in device functionalities.
- Integrating CMQWs with emerging 2D materials could create nearly isotropic high $\chi^{(2)}$ systems, expanding design possibilities.
- Optimizing metasurface design for specific applications, such as enhancing polarization components or achieving directional SHG emission, is a potential research avenue.
- Overall goal: miniaturizing and integrating these materials into practical nonlinear optical devices for applications in frequency conversion, signal processing, and optical communication.
- Integrating high $\chi^{(2)}$ QWs with photonic devices on a chip scale could lead to efficient nonlinear optical components.
- Engineering QW heterostructures for broader bandwidth nonlinear effects holds promise.
- Combining QWs with plasmonic enhancements could further improve the efficiency of nonlinear effects in future devices.

8. Reference

- [1] <https://onlinelibrary.wiley.com/doi/10.1002/adfm.202000829>
- [2] <https://pubs.aip.org/aip/apl/article-abstract/116/24/241105/986102/Large-second-order-nonlinearity-in-asymmetric?redirectedFrom=fulltext>
- [3] https://www.researchgate.net/publication/342228447_Large_second-order_nonlinearity_in_asymmetric_metallic_quantum_wells
- [4] <https://www.nature.com/articles/s41377-019-0123-4>
- [5] https://www.researchgate.net/publication/341417245_Nanoscale_optical_pulse_limiter_enabled_by_refractory_metallic_quantum_wells
- [6] https://www.researchgate.net/publication/282209625_Investigation_of_the_reflection_and_transmission_of_nano-scale_gold_films
- [7] Agrawal, G. Nonlinear Fiber Optics. 5th edn, (Elsevier, New York, 2012).
- [8] <http://advances.sciencemag.org/content/suppl/2020/05/11/6.20.eaay3456.DC1>
- [9] M. Sheik-Bahae, A. A. Said, T. H. Wei, D. J. Hagan, E. W. V. Stryland, Sensitive measurement of optical nonlinearities using a single beam. IEEE J. Quantum Electron. 26, 760–769 (1990)
- [10] <https://www.science.org/doi/10.1126/science.1205771>
- [11] <https://ieeexplore.ieee.org/document/142553>
- [12] <https://iopscience.iop.org/article/10.1088/0022-3719/20/36/020>